Terephthalamide Ring Dynamics of Poly(*p*-phenyleneterephthalamide)‡

R. J. Schadt,† E. J. Cain, K. H. Gardner, V. Gabara, S. R. Allen, and A. D. English*

DuPont Central Research and Development and DuPont Fibers, Experimental Station, Wilmington, Delaware 19880-0356

Received April 19, 1993; Revised Manuscript Received August 5, 1993®

ABSTRACT: The dynamics of terephthalamide rings in poly(*p*-phenyleneterephthalamide) (PPTA) are examined with ^2H NMR spectroscopy, and a description of motion at this site is developed in conjunction with crystallite size information from X-ray diffraction data, thermal expansion data, and ^2H NMR results for the amide and *p*-phenylenediamine ring sites. Spin–lattice relaxation results for the terephthalamide rings differentiate those sites in proximity to non-hydrogen-bonded amide sites on crystallite surfaces from those sites near hydrogen-bonded amides on both the crystallite surfaces and interior. The evolution of the fraction of terephthalamide rings which execute a π-flipping motion as a function of temperature reflects the dynamic heterogeneity at this site; this process is reflective of not only the proximity of mobile amide sites on the crystallite surface but also the extent of structural imperfection.

Introduction

Poly(*p*-phenyleneterephthalamide), PPTA, is a highly crystalline[1] aromatic polyamide that can exist in two crystal modifications, denoted as I (Northolt[2]) and II (Haraguchi[3]), depending upon the conditions of precipitation.[4] While the unit cells of both polymorphs have been characterized, the type of chain motion and its relationship to the morphology and crystallite perfection have been controversial.[5-9] Knowledge of the dynamic structure and its relationship to the primary chemical structure and fiber morphology is of utility in understanding structural accessibility[10] and biopersistence.[11]

The idealized structure of PPTA fibers consists of radially stacked hydrogen-bonded sheets of aramid molecules which are organized into pleated sheet structures which are nearly parallel to the fiber axis.[12] A schematic representation of PPTA molecules in a hydrogen-bonded sheet is illustrated in Figure 1. From a structural perspective this material is thought to contain virtually no amorphous material,[1,13] but the crystalline character has been shown to be structurally heterogeneous, as characterized by crystallite perfection and size.[14] More recently, a ^2H NMR study[15,16] of the dynamics of amide sites in N-deuterated PPTA, in combination with X-ray diffraction and transmission electron microscopy, has revealed that the dynamic structure is quite heterogeneous and the crystallite surfaces or defect regions are dynamically differentiated from the crystallite interior. In the paper following this one, a ^2H NMR investigation of diamine ring deuterated PPTA reveals further details of the dynamic structure[17] of PPTA. In this paper we focus on the dynamics of the terephthalamide rings in PPTA.

Previous ^1H and ^{13}C NMR studies[5,6] of PPTA have interpreted their experimental results from a dynamically homogeneous perspective, where the motion of each chemically distinct site is considered to be essentially identical, and have concluded that the aromatic rings exhibit restricted motion. There is some ^{13}C NMR data indicating that the presence of water may affect the local symmetry of the terephthalamide rings and that there may be a small noncrystalline-like fraction which has low flexibility, absorbs water, and is identified through its spin–lattice relaxation time.[7] Preliminary results concerning the nature of terephthalamide ring motion for both PPTA polymorphs have been reported in a ^2H NMR study[8,9] of the polymer in which half of the terephthalamide rings were perdeuterated. These results indicated that only a fraction of the terephthalamide rings were able to flip at an appreciable rate over a wide temperature range and the fraction increased slowly and monotonically with temperature; this behavior indicated a large degree of *dynamic heterogeneity* of the terephthalamide ring sites in PPTA for both polymorphs. We present here a more complete ^2H NMR study of the terephthalamide ring dynamics of PPTA to gain further insight into the nature of the dynamic heterogeneity in this system and its relationship to the structural heterogeneity.

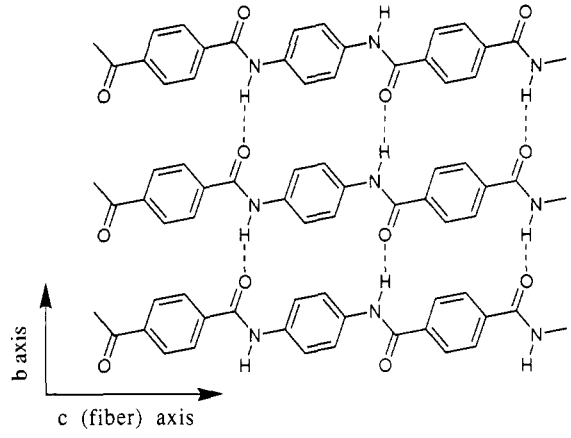

Figure 1. Schematic diagram of PPTA molecules in a hydrogen-bonded sheet.

Experimental and Calculational Procedures

Polymer Preparation. Terephthalamide ring perdeuterated PPTA with an inherent viscosity of 2.7 dL/g and number-average molecular weight of 10 kg/mol was prepared by copolymerizing *p*-phenylenediamine with 99+% isotopically pure terephthaloyl-d_4 chloride in *N*-methylpyrrolidone.[18] PPTA with half of the terephthalamide rings perdeuterated (hemideuterated PPTA), inherent viscosity of 4.3 dL/g and number-average molecular

* To whom correspondence should be addressed.
† Current address: Polymer Division, Building 224, Room A209, NIST, Gaithersburg, MD 20899.
‡ Contribution No. 6451.
® Abstract published in *Advance ACS Abstracts,* October 15, 1993.

0024-9297/93/2226-6503$04.00/0

weight of 16 kg/mol, was produced by copolymerizing *p*-phenylenediamine with an equimolar mixture of terephthaloyl chloride and deuterated terephthaloyl chloride. Though the inherent viscosities of the deuterated polymers are smaller than that found for commercially-available PPTA,[1] the number-average molecular weights are still appreciable. Polymorph I was obtained by coagulation of a sulfuric acid solution in water at ambient temperature. A mixture of polymorphs I and II was obtained via extraction of H_2SO_4 in chilled water from a PPTA/H_2SO_4 crystallosolvate.[4]

PPTA fiber was air gap spun from an 18.5% solution of the hemideuterated PPTA in 100% H_2SO_4 into a cold water bath and air-dried at room temperature, resulting in physical properties of 5.8 denier, 12 g/d (1.5 GPa) tenacity, 4.2% ultimate elongation, and 300 g/d (39 GPa) modulus. Subsequent vacuum drying at 200 °C for 17 h produced a fiber with modified physical properties: 14 g/d (d = denier) (1.8 GPa) tenacity, 3% ultimate elongation, and 475 g/d (60 GPa) modulus. These physical properties may be compared to those reported for Kevlar 29 [23 g/d tenacity (3 GPa), 3.6% ultimate elongation, 480 g/d (62 GPa) modulus)] and Kevlar 49 [(23 g/d (3 GPa) tenacity, 2.5% ultimate elongation, 910 g/d (117 GPa) modulus].[19] [The fiber was not prepared from terephthalamide ring perdeuterated PPTA because of its low inherent viscosity.] Chopped fiber samples were prepared for the NMR experiments by cutting the fiber into ~1-mm pieces and packing in a 5-mm NMR tube. X-ray diffraction measurements (see next section) indicate that the cut fiber sample packed into the NMR tube is quite close to being isotropically dispersed. Given the relative insensitivity of NMR to this level of orientation,[20] the sample is subsequently treated as being isotropic.

X-ray Diffraction Measurements. Variable temperature X-ray diffractometry scans were collected in the symmetrical reflection mode using an automated Scintag Model XDS 2000 θ–θ diffractometer (curved crystal monochromator, 1° divergence and receiving slits) equipped with a high temperature stage and Cu Kα radiation. Data were collected in a fixed time mode with a step size of 0.05° from 4 to 50° 2θ at room temperature and over the range 60–240 °C in 20-deg intervals. The sample temperature was measured by a thermocouple embedded in the sample.

X-ray diffraction patterns were recorded for the chopped fiber NMR sample using a flat plate vacuum camera with Cu Kα radiation; the data were digitized with a Photomation P-1700 (Optronics International). The chopped fiber sample was removed intact from the NMR tube and a disk was cut from the center of the cylinder from which a center 1-mm-thick section was cut for X-ray analysis. Values for the intensity versus angle (with respect to the NMR tube axis) were extracted from the digitized image for the 110 and 200 reflections; additionally, radial scans were used to determine the background intensity. The orientation parameter, $\mathbf{F}_{c,\text{NMR tube axis}}$, defines the orientationof the crystallographic *c* axis with respect to the NMR tube axis. $\mathbf{F}_{c,\text{NMR tube axis}}$ was experimentally determined to be equal to –0.098, indicating that the sample is essentially isotropic with a very slight preferred orientation of the chain axis direction normal to the NMR tube axis.

PVT Measurements. Pressure–volume–temperature measurements[21] were acquired over a pressure range of 0–200 MPa and a temperature range of 30–390 °C using a 1.5-g sample of nondeuterated PPTA fiber (Kevlar 29). TGA analysis revealed that drying at temperatures above 300 °C removed more than 95% of the water; therefore, the fiber was dried in the *PVT* cell at 308 °C in a vacuum oven with a nitrogen purge for 72 h prior to measurements.

NMR Measurements. Fully- and partially-relaxed ^{2}H NMR spectra and associated spin–lattice relaxation data were obtained over a temperature range of –79 to +228 °C with a Bruker MSL 200 spectrometer operating at a resonance frequency of 30.72 MHz using a previously described procedure.[22] ^{2}H NMR spectra were acquired using a quadrupolar echo pulse sequence with a delay time of 40 μs between 90° pulses for perdeuterated and hemideuterated polymorph I polymer, hemideuterated mixed polymorph polymer, and hemideuterated polymorph I chopped fibers. As previously described, the orientational dependence of the NMR measurements of the hemideuterated polymorph I fiber was eliminated by preparing a chopped fiber sample. ^{2}H NMR spectra over the temperature range –38 to +118 °C, for both perdeuterated polymorph I polymer and hemideuterated mixed polymorph polymer, were acquired using delay times of 20, 40, 80, and 160 μs between quadrature pulses.

NMR Line Shape Simulation. NMR line shape simulations were carried out, as previously described,[22] that allowed for restricted angle rapid fluctuations (rapid liberational motion) about the 1,4 axis of the terephthalamide ring in addition to a variable rate π-flip about the same axis. The model which best fits the experimental data uses a dual population of correlation times for the ring-flipping process, with a nearly rigid component assigned a $\tau_c > 0.1$ s and a rapidly flipping component assigned a $\tau_c < 1.0 \times 10^{-9}$ s. Alternatively, the experimental spectra could be *assumed* to result from a very broad distribution of correlation times which would produce line shapes that cannot be differentiated from those produced by the bimodal population model.

Results and Discussion

As-Polymerized Polymer. It is well-known that the dynamics of individual polymer segments differ quite markedly when located in domains of different morphology. For semicrystalline polymers this is minimally described by a two phase model of crystalline and amorphous domains. For PPTA our interest is to develop a detailed model of the dynamic structure of the terephthalamide rings and to investigate how this is affected by the presence of polymorphism and the additional structural perfection provided by fiber spinning.

We previously reported in a preliminary communication[9] that the ^{2}H NMR line shapes of crystal modification I are quite similar to those obtained for a sample composed of 60% modification II and 40% modification I (composition estimated from the characteristic X-ray diffraction peaks for each modification). The temperature dependent line shapes for the mixed modification material, as compared to pure modification I, differ primarily in that there is an offset of approximately 10 °C to lower temperature. This would indicate that the terephthalamide rings in modification II are somewhat more mobile than in modification I at a given temperature. The substantial similarity of the temperature dependences of the line shapes for the terephthalamide rings in modifications I and II may reflect the identical densities of the two modifications, as calculated from the unit cell parameters.[3] Due to the complexities of the model used to simulate the NMR data for the pure modification I polymer and our inability to produce a macroscopic sample of pure modification II polymer, no further attempt was made to analyze these data.

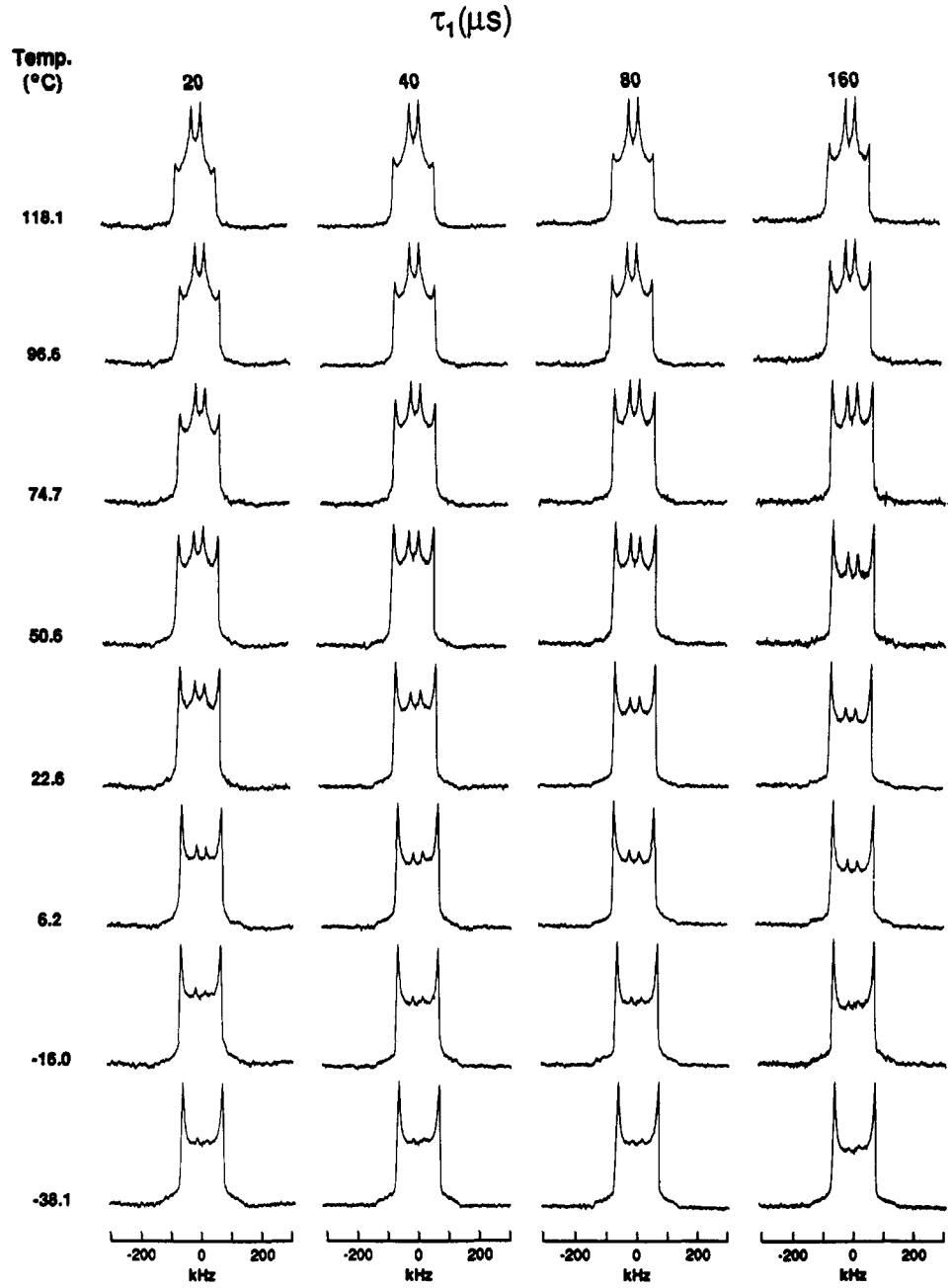

Figure 2. Experimental ^2H NMR line shapes for a PPTA (PPD/T(d_4)) polymer in crystal modification I as a function of temperature and delay between quadrature radio frequency pulses.

Figure 2 illustrates the experimental ^2H NMR line shapes for PPTA in polymorph I as a function of both temperature and delay between quadrature radio frequency pulses. (Anisotropic line shape distortions as a function of the delay between quadrature pulses are used to detect the presence of a significant population undergoing an intermediate rate exchange process with a characteristic lifetime near $\tau_c \sim 10^{-4}$ s). These data illustrate that only over the narrow temperature interval of 23–97 °C is there any detectable dependence of the line shapes on the refocusing time. This observation indicates that to a good approximation the line shapes represent either a population distribution which is bimodal, in that either the terephthalamide rings flip slowly ($\tau_c > 10^{-2}$ s) or rapidly ($\tau_c < 10^{-7}$ s) at all accessible temperatures, or a population distribution which is a continuous distribution which does not have a significant population (20%) in the intermediate rate regime.[23] Given the sparsity of the data indicating any dependence of the line shapes on refocusing time, we chose to use the bimodal population model[9] as the simplest model consistent with the vast majority of the data. Attempts to separate the contributions to the line shape from π-flipping and non-π-flipping components via spin–lattice relaxation time discrimination were not successful in that it is not possible to completely isolate either the π-flipping or the non-π-flipping component in either the slower or more rapidly relaxing T_1 component. This observation indicates that the process responsible for the partitioning of the magnetization into two well separated components in the T_1 measurements is *not* the π-flipping process. The process primarily responsible for the T_1 discrimination is due to enhanced mobility of some sites on the crystallite surfaces, and this process is more fully explored in the paper following this one and elsewhere.[16] Nevertheless, the very great temperature range (>300 °C)[9] required for the line shape to evolve from one with essentially no π-flipping component to one where essentially the whole line shape is represented by a π-flipping component indicates that this is not a single simple unimolecular process. As we reported previously,[9] analysis[24] of the temperature dependence of the fraction of the line shape represented as a π-flipping component

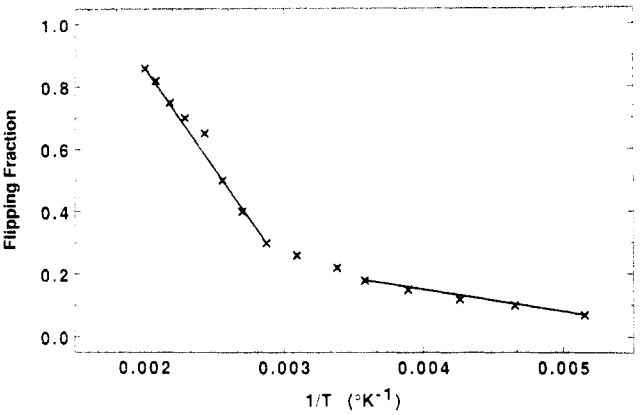

Figure 3. Temperature dependence of the fraction of rapidly π-flipping terephthalamide rings in PPTA polymer.

by assuming that a process described by a Gaussian distribution of activation energies is responsible for the experimental observations would predict that the distribution would be centered at ~12 kcal/mol and have a full width at half-maximum of ~8 kcal/mol. This simple interpretation is obviated by our observations of the dynamics of the amide sites in PPTA[15,16] which indicate that to a first approximation the populations are differentiated into two components associated with crystallite surfaces and interior. Figure 3 illustrates that when the fraction of π-flipping terephthalamide rings is plotted as a function of reciprocal temperature it appears as though two regimes exist. The low temperature regime, with the smaller slope, appears to represent ~25% of the population; the remainder of the population appears in the higher temperature regime and has a larger slope. These data are consistent with the model developed from the amide sites where a minor fraction of the sites (~25%) exhibit large amplitude mobility at all accessible temperatures (−184 to +228 °C), and the majority of the population exhibits no large angle reorientation over this entire temperature range. Thus to first order, it appears that the terephthalamide rings are described by two populations, with the minor population constituting ~25% and evidently characterized by a less energetic process (either in terms of an activation energy for the process or a free energy difference associated with generation of free volume to allow a π-flipping motion) than the high temperature population.

Additional experimental evidence for such a model is available from estimates of the characteristic crystallite size of the PPTA polymer. Figure 4 illustrates a representation of the average crystallite size in the plane normal to the chain axis determined from the width of the X-ray diffraction peaks. Scherrer analysis of the X-ray data indicated that the average crystallite dimension in the *ab* plane was approximately 30–35 Å and that the outline of the crystallite cross-section could be qualitatively represented as circular. Crystallites of this size have approximately 40% of their chains on the surface of the crystal. Approximately half of the amide sites in the chains on the crystallite surfaces cannot hydrogen bond; hence approximately 20% of the amide sites in the entire crystallite will have a very different static structure and, as observed,[15,16] dynamic structure. (Note that Figure 1 illustrates that only half of the C=O or N—H sites in a chain located on the edge of hydrogen-bonded sheet are proximate to another molecule with which they may form a hydrogen bond.) These observations correlate nicely with the observed temperature dependence of the fraction of π-flipping terephthalamide rings. The minor fraction of

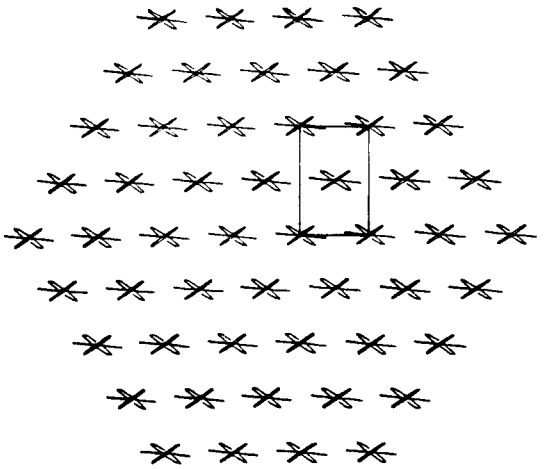

Figure 4. Schematic of the crystallite cross-sectional dimensions of as-polymerized PPTA (*ab* plane of the indicated unit cell) in crystal modification I. Note that the *a* axis is vertical and the *b* axis is horizontal and is coincident with the hydrogen-bonding direction.

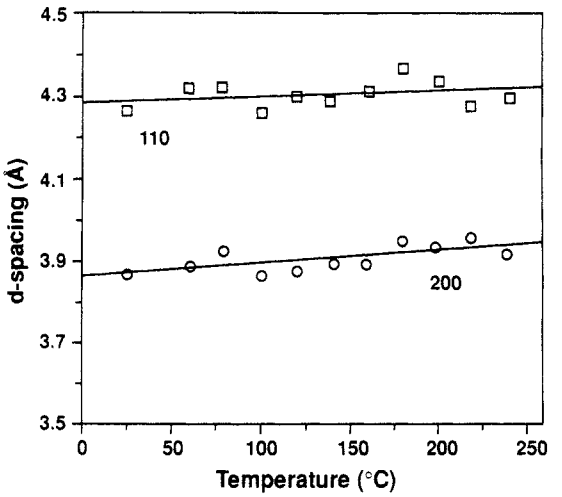

Figure 5. Temperature dependence of the (110) and (200) X-ray diffraction peaks for as-polymerized PPTA.

sites, which begin to flip at lower temperature, may be associated with terephthalamide rings near non-hydrogen-bonded amide sites on the crystallite surface. The major fraction may be associated with terephthalamide rings near hydrogen-bonded amide sites on both the crystallite surface and interior where activation of the π-flipping process is surely more difficult due to more perfect molecular packing than at non-hydrogen-bonded surface sites.

Further evidence for the nature of the populations associated with the surface and interior of crystallites was sought from examination of the thermal expansion coefficients determined from both X-ray diffraction and pressure dilatometry. Figure 5 illustrates the temperature dependence of the X-ray diffraction peak positions for the 110 and 200 reflections. While the *d* spacing for the 200 reflection showed a substantial change in spacing with temperature ($\alpha_{200} = 8.90 \times 10^{-5}$ °C^{-1}), the position of the 110 reflection was substantially less affected ($\alpha_{110} = 3.28 \times 10^{-5}$ °C^{-1}). Figure 6 displays the change in the *a* and *b* lattice parameters as a function of temperature derived from these reflections; $a = 2d_{200}$, $b^{-2} = [(1/d_{110})^2 - (1/a^2)]$. The *b* axis corresponds to the distance between chains in the hydrogen-bonded sheet and is essentially invariant with temperature (note the near equivalence of the zero slope (dotted) line and the least squares (solid) line fit to

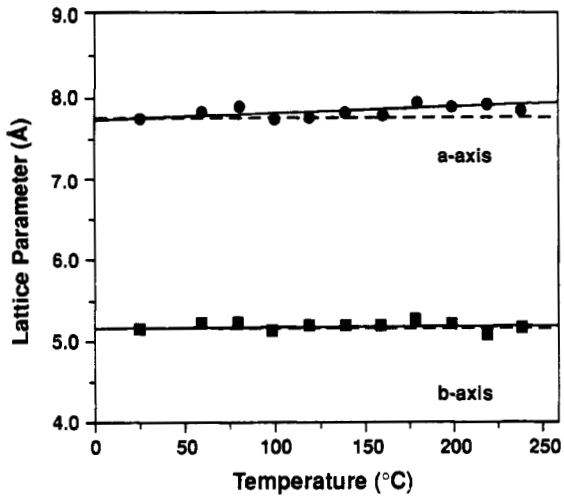

Figure 6. Temperature dependence of the a and b lattice parameters of the as-polymerized PPTA polymer. The dotted lines have a slope of zero, and the solid lines are a least squares fit through the data.

Table I. Thermal Expansion Coefficients ($°C^{-1}$) for PPTA (Modification I)

	PPTA polymer	PPTA fiber[a]
α_a	8.90×10^{-5} ($R = 0.69$)	8.3×10^{-5}
α_b	0.90×10^{-5} ($R = 0.07$)[b]	4.7×10^{-5}
α_c		-2.9×10^{-6}
α_{vol}	9.5×10^{-5}	1.27×10^{-4}

[a] From ref 25. [b] R: Pearson product moment correlation coefficient.

the data), whereas the a axis direction, which corresponds to the van der Waals packing of hydrogen-bonded sheets, shows significant expansion with temperature (note the divergence of the solid and dotted lines with temperature). Table I compares values of the thermal expansion coefficient derived from this work on the PPTA polymer to that previously reported for oriented fibers.[25] The volume thermal expansion coefficient for the PPTA polymer is estimated from the values of α_a and α_b from this work and the value of $\alpha_c = -2.9 \times 10^{-6}$ °C^{-1} [25] to be $\alpha_v = 9.5 \times 10^{-5}$ °C^{-1}, and this value may be compared to that found[25] for PPTA fibers where $\alpha_v = 1.27 \times 10^{-4}$ °C^{-1}. From this examination of the thermal expansion coefficient of the as-polymerized polymer compared to the fiber, we find surprisingly that the fiber apparently has a somewhat larger coefficient of thermal expansion. Also, we find no evidence of two distinct regimes with substantially different thermal expansion coefficients; hence, this indicates that the two types of sites differentiable by NMR spin–lattice relaxation are not differentiable via their thermal expansion coefficients. Again this is consistent with the sites being associated with crystallite surface and interior.

Finally, a bulk macroscopic coefficient of thermal expansion for the PPTA fiber was calculated from the PVT data for comparison to the value of the microscopic thermal expansion coefficient obtained from X-ray measurements. This calculation consisted of a linear least squares analysis of specific volume vs temperature for each of several isobars in the range from 20 to 100 MPa. Slopes of each of these isobars were then plotted vs pressure, and a second linear least squares analysis was performed. The resulting fitted line was extrapolated to zero pressure, and a value for the slope of specific volume vs temperature at zero pressure was obtained. This value was divided by the specific volume at room temperature to yield α_v. The macroscopic coefficient of thermal expansion was determined to be 1.182×10^{-4} °C^{-1} for the temperature range 30–120 °C and 1.551×10^{-4} °C^{-1} for the temperature range

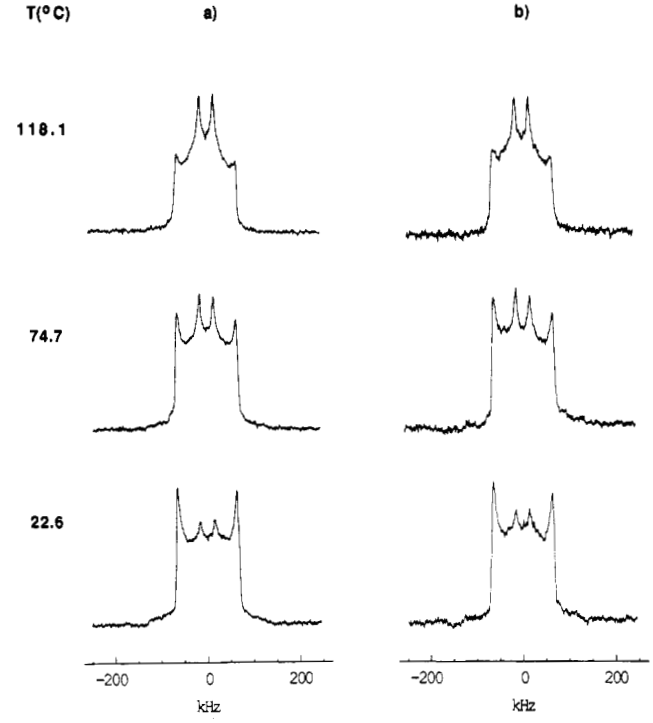

Figure 7. Experimental ^2H NMR line shapes, delay between quadrature pulses of 40 μs, for PPTA (PPD/T(d_4)) in crystal modification I as a function of temperature for both as-polymerized polymer (a) and chopped fiber (b).

135–300 °C. These values are quite close to those previously calculated from the fiber X-ray data[25] and once again indicate that either the polymer is very highly crystalline or that any noncrystalline component has a thermal expansion coefficient very close to that of the crystal. Neither of these results give any direct evidence of a dual population model, but this is not surprising given the proposed morphological origin of these populations.

PPTA Fiber. Figure 7 illustrates a comparison of the ^2H NMR spectra of the PPTA (PPD/T(d4)) polymer (modification I) for both as-polymerized and fiber forms. These results indicate that the ^2H NMR line shapes of the terephthalamide rings are not sensitive to the type of fiber forming process employed here. Furthermore, the spin–lattice relaxation values obtained for the chopped fiber sample are essentially identical within experimental error to that found for the as-polymerized polymer. Hence, the process of fiber formation for PPTA utilized here plays no significant role in modifying the dynamics of the terephthalamide rings. The observed insensitivity of the NMR results to fiber formation is due to the fraction of sites located on the crystallite surfaces being quite similar for the as-polymerized polymer and the fiber. This result once again reflects the relative insensitivity of the terephthalamide ring π-flipping mode to the morphology; whereas, the terephthalamide ring spin–lattice relaxation data, the amide data, and the diamine ring data do reflect the effect of the morphology (crystallite size) on the local segmental dynamics.

Conclusions

The crystallite size perpendicular to the chain axis of as-polymerized PPTA is shown by X-ray diffraction to be quite small with a characteristic dimension of 30–35 Å. For crystals of this size, a large fraction (~40%) of all chains reside on the surface and hence ~20% of all amide sites in the entire crystal are not capable of forming a hydrogen bond. Concomitantly, ~25% of all terephthalamide rings are differentiated by their low temperature

rapid spin–lattice relaxation rate from the majority of sites; this relaxation process is evidently attributable to the motion of the N–H bonds.[16] Additionally, this process is evidently the origin of the ^{13}C NMR spin–lattice relaxation results which were attributed to a "semicrystalline" model.[7]

The observation of two apparent regimes of mobilization of the π-flipping motion of the terephthalamide rings is thought to be related to a bimodal population distribution where those sites which may more easily execute this motion (surface sites near non-hydrogen-bonded amide sites) constitute the minority ($\sim$25%) and the majority population is associated with sites near hydrogen-bonded amide sites on either the crystallite surface or interior. For both populations, the very large temperature interval that is necessary to enable each population to become fully able to execute a π-flip is attributable to the dynamic nonuniformity or heterogeneity of this system. This model is supported by other ^2H NMR data for both amide sites and *p*-phenylenediamine rings, X-ray data, and thermal expansion coefficients.

Terephthalamide rings in modification I polymorph appear from their ^2H NMR line shapes to have a slightly lower degree of mobility than those situated in polymorph II. Additionally, terephthalamide rings in modification I polymorph are insensitive to the type of fiber spinning employed in this investigation. This insensitivity to fiber formation reflects the small change in crystallite size (hence the population of crystallite surface sites) associated with the spinning process utilized here.

Acknowledgment. We are indebted to P. A. Cooper and B. J. Haley for skilled technical assistance.

References and Notes

(1) Panar, M.; Avakian, P.; Blume, R. C.; Gardner, K. H.; Gierke, T. D.; Yang; H. H. *J. Polym. Sci., Polym. Phys. Ed.* **1983**, *21*, 1955.
(2) Northolt, M. G. *Eur. Polym. J.* **1974**, *10*, 799.
(3) Haraguchi, K.; Kajiyama, T.; Takayanagi, M. *J. Appl. Polym. Sci.* **1979**, *23*, 915.
(4) Roche, E. J.; Allen, S. R.; Gabara, V.; Cox, B. *Polymer* **1989**, *30*, 1776.
(5) English, A. D. *J. Polym. Sci., Polym. Phys. Ed.* **1986**, *24*, 805.
(6) Hong, J.; Harbison, G. S. *Polym. Prepr. (Am. Chem. Soc., Div. Polym. Chem.)* **1990**, *31*, 115.
(7) Fukuda, M.; Kawai, H.; Horii, F.; Kitamaru, R. *Polym. Commun.* **1988**, *29*, 97.
(8) Cain, E. J.; Gardner, K. H.; Gabara, V.; Allen, S. R.; English, A. D. *Polym. Prepr. (Am. Chem. Soc., Div. Polym. Chem.)* **1990**, *31*, 518.
(9) Cain, E. J.; Gardner, K. H.; Gabara, V.; Allen, S. R.; English, A. D. *Macromolecules* **1991**, *24*, 3721.
(10) Ozawa, S. *Polym. J.* **1987**, *19*, 119.
(11) Warheit, D. B.; Kellar, K. A.; Hartsky, M. A. *Toxicol. Appl. Pharmacol.* **1992**, *116*, 225.
(12) Dobb, M. G.; Johnson, D. J.; Saville, B. P. *J. Polym. Sci., Polym. Phys. Ed.* **1977**, *15*, 2201.
(13) Tashiro, K.; Kobayashi, M.; Tadokoro, H. *Macromolecules* **1977**, *10*, 413.
(14) Dobb, M. G.; Johnson, D. J.; Saville, B. P. *J. Polym. Sci., Polym. Symp.* **1977**, *58*, 237.
(15) Schadt, R. J.; Cain, E. J.; Gardner, K. H.; Gabara, V.; Allen, S. R.; English, A. D. *Polym. Prepr. (Am. Chem. Soc., Div. Polym. Chem.)* **1991**, *32*, 253.
(16) Jackson, C. L.; Schadt, R. J.; Gardner, K. H.; Chase, D. B.; Allen, S. R.; Gabara, V.; English, A. D. *Polymer*, in press.
(17) English, A. D.; Gardner, K. H.; Schadt, R. J.; Cain, E. J.; Gabara, V.; Allen, S. R. *Polym. Prepr. (Am. Chem. Soc., Div. Polym. Chem.)* **1992**, *33*, 82.
(18) Tanner, D.; Fitzgerald, J. A.; Phillips, B. R. *Adv. Mater.* **1989**, *5*, 151.
(19) Yang, H. H. *Aromatic High Strength Fibers*; SPE Monographs; Wiley-Interscience: New York, 1989.
(20) Simpson, J. H.; Rice, D. M.; Karasz, F. E. *Macromolecules* **1992**, *25*, 2099.
(21) Zoller, P.; Bolli, P.; Pahud, V.; Ackermann, H. *Rev. Sci. Instrum.* **1976**, *47*, 948.
(22) Hirschinger, J.; Miura, H.; Gardner, K. H.; English, A. D. *Macromolecules* **1990**, *23*, 2153.
(23) Schadt, R. J.; Cain, E. J.; English, A. D. *J. Phys. Chem.* **1993**, *97*, 8387.
(24) Rössler, E.; Taupitz, M.; Börner, K.; Schulz, M.; Vieth, H. M. *J. Chem. Phys.* **1990**, *92*, 5847.
(25) Tadaoki, I.; Tashiro, K.; Kobayashi, M.; Tadokoro, H. *Macromolecules* **1986**, *19*, 1772.